

# COHERENT SYNCHROTRON OSCILLATION EXCITED BY A RIPPLE OF A KLYSTRON POWER SUPPLY

M. Hara, T. Nakamura, T. Ohshima, T. Takashima, SPring-8, Kamigori, Japan

## Abstract

Coherent synchrotron oscillation was observed in the SPring-8 storage ring as sidebands at the harmonics of the accelerating frequency, which is independent of beam current. This is explained using a forced oscillation model of the synchrotron oscillation by the disturbance of accelerating voltage. The RF disturbance is induced by the ripple noise in the klystron power supply at the harmonics of the frequency of the AC power supply.

## 1 INTRODUCTION

If a klystron power supply has excessive ripple noise, electron beams accelerated by a cathode voltage in the klystron suffer from ripple effects that modulate their velocities, and, as a consequence, amplified RF is modulated. If one of the frequency components is close to the synchrotron oscillation frequency, the ripple noise induces a coherent synchrotron oscillation.

The ripple noise effects in the SPring-8 storage ring, were measured by varying the effective accelerating voltage. These effects were found in a sideband signal of the accelerating frequency (508.58 MHz) from a pickup electrode of the ring; and the sideband signal frequency was a higher harmonic of the AC power supply ( *i.e.*, multiples of 360 Hz).

The effect of RF phase noises on the electron beam were recently investigated theoretically[1]. In the SPring-8 storage ring, coherent synchrotron oscillation caused by high voltage ripples in the klystron was found to be a sideband peak of the acceleration frequency [2]; and the strength of the sideband can be explained by a simple forced oscillation model.

## 2 PHASE DELAY IN KLYSTRON

In a klystron, electrons are emitted from a cathode and accelerated by a cathode-collector voltage and captured by a collector. Electrons are velocity-modulated by the input cavity, which is excited at RF frequency, and pass through drift space. On the way to the collector, the electrons are bunched by velocity modulation; and the bunched electrons induce the RF voltage in the output cavity.

Slight voltage change in the cathode affects the electron travel time and causes a phase delay in the RF output. The voltage fluctuation ( $\Delta V_k / V_k$ ) coefficient for the phase delay is calculated [2].

$$D \equiv V_k \frac{d\theta_D}{dV_k} = -2\pi f_{RF} \frac{L}{c} \frac{1}{(\beta\gamma)^3} \frac{eV_k}{m c^2} \quad (1)$$

where:  $f_{RF}$  is the RF frequency;  $L$  the length between the input cavity and the output cavity;  $\beta$  the dimensionless velocity of the electron beam;  $c$  the velocity of light;  $\gamma$  the dimensionless energy of the electron beam;  $-V_k$  the

cathode voltage;  $e$  electron charge; and  $mc^2$  the electron rest mass energy.

In the SPring-8 case, where  $L = 2.5$  m,  $f_{RF} = 508.58$  MHz, and  $V_k = -80$  kV, a ripple noise of  $\Delta V/V = 10^{-3}$  induces a phase difference of  $1.2^\circ$ . This is comparable to the bunch length  $\sigma_\theta = 2.44^\circ$  in the SPring-8 storage ring.

## 3 BUNCH RESPONSE

The equation for small phase oscillations  $\tau$  in a bunch is given by [3],

$$\frac{d^2\tau}{dt^2} + 2\alpha_\epsilon \frac{d\tau}{dt} + \Omega^2\tau = 0, \quad (2)$$

where  $\alpha_\epsilon$  is damping coefficient,  $\Omega$  is the synchrotron oscillation (angular) frequency. The phase modulation affects  $\Omega^2$  through  $V_{RF}$ . This modulation can be treated as an external force in a simple forced oscillation model.

$$\frac{d^2\tau}{dt^2} + 2\alpha_\epsilon \frac{d\tau}{dt} + \Omega^2\tau = \frac{\Omega^2}{\omega_{RF}} \Delta\theta_D e^{j\omega t} \quad (3)$$

Solution of eq(3) can be expressed as

$$\tau = \frac{\frac{\Omega^2}{\omega_{RF}} \Delta\theta_D e^{j\omega t}}{\sqrt{(\Omega^2 - \omega^2)^2 + 4\alpha_\epsilon^2 \Omega^2}}. \quad (4)$$

A ripple with angular frequency  $\omega$  in a klystron power supply induces synchrotron oscillation with amplitude expressed by eq(4). If the accelerating voltage is changed for a fixed  $\omega$ , the amplitude is maximum at  $\Omega = \omega$  and the peak value is proportional to  $\Omega$ .

## 4 SYNCHROTRON OSCILLATION AMPLITUDE

It is well known that particle longitudinal signal from a single particle at time  $t$  and angular azimuth position  $\theta$  can be described as [4]

$$s_{//}(t, \theta) = e^{-\sum_{n=-\infty}^{\infty} \delta(t - \tau - \frac{\theta}{\omega_0} - \frac{2n\pi}{\omega_0})}, \quad (5)$$

where:  $\delta$  is the Dirac function;  $\tau$  the time interval between the reference particle passing and test particle passing; and  $\omega_0$ , the angular revolution frequency. With the Fourier transform, the spectrum is a line spectrum at frequencies  $\omega_{pm}$  ( $= p\omega_0 + m\omega_{s0}$ )

$$s_{//}(\omega, \theta) = \frac{e^{-j\omega\theta}}{2\pi} \sum_{p,m=-\infty}^{\infty} j^{-m} J_m(p\omega_0\bar{\tau}) e^{-j(p\theta - m\psi_0)} \delta(\omega - \omega_{pm}) \quad (6)$$

where  $J_m(x)$  is a Bessel function,  $\psi_0$  the synchronous phase at  $t = 0$ ,  $\omega_{s0}$  and  $\bar{\tau}$  are the synchrotron oscillation frequency and amplitude.

The spectrum amplitude at the revolution frequency and the first sideband are described as

$$S_{0s}(p) = I J_0(p\omega_0\bar{\tau}), \quad (7)$$

$$S_{1s}(p) = I J_1(p\omega_0\bar{\tau}), \quad (8)$$

where  $I$  is the electron current and  $p$  is an integer. power spectrum ratio is given as

$$R_s(p) = \left( \frac{S_{1s}(p)}{S_{0s}(p)} \right)^2 = \left( \frac{J_1(p\omega_0\bar{\tau})}{J_0(p\omega_0\bar{\tau})} \right)^2. \quad (9)$$

Using this single particle model, excited synchrotron oscillation amplitude can be estimated.

## 5 MEASUREMENT

In the SPring-8 storage ring, three RF stations (B, C, D) are installed and each station has 8 single-cell cavities which are powered by 1 MW klystron. The maximum voltage and current of the klystron power supply is 90 kV and 20 A, and the AC power line frequency is 60 Hz.

The power supply is thyristor regulated and has no crowbar circuit and no large capacitor bank [5]. Each power supply is a six-phase rectifier circuit (with ripple noises occurring at multiples of 360 Hz): and the klystron power supplies in the three stations are phase-shifted by  $20^\circ$  from each other at their input transformer. Therefore, if each station is finely tuned and three stations are balanced, equivalent 18-phase rectifier could be expected (with ripple noises in multiples of 1080 Hz). In fact, there are some causes that disturb the balances, so that the extra harmonic components are excited in the power supply. An example of the ripple measurements on the cathode voltage using an FFT analyzer is shown in Fig. 1. In this case, frequency components in multiples of 360 Hz can be seen at the level  $\Delta V/V \approx 10^{-3}$ . Frequency components of 60 Hz, 180 Hz, 540 Hz etc., were also observed in the output, which comes from the above stated unbalance.

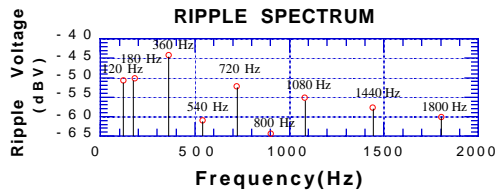


Figure 1: An Example of the power supply ripple noise spectrum below 2 kHz in D station.  $V_k = -60$  kV.

The electron beam signal from a Beam Position Monitor (BPM) electrode was measured at the acceleration frequency (508.58 MHz). Sideband signal is investigated varying the effective cavity voltage in two ways.

### 5.1 First measurement

Cavity voltages (measured by the pickups attached to the cavities and vector summed) at three stations (B, C, and D) were kept constant (set voltages were  $V_b = 5.13$  MV,  $V_c = 4.89$  MV and  $V_d = 3.54$  MV after calibration), and the phase of the B station ( $\theta_b$ ) was varied. In this way, effective cavity voltage was varied without changing station voltage. Therefore klystron power supply was kept constant. Stored currents were about 200  $\mu$ A.

The power spectrum was measured using spectrum analyzer (HP8591E) and an example of the raw data is shown in Fig. 2. We can see the sideband peaks of the coherent synchrotron oscillation around the acceleration frequency. Observed sideband peak frequencies were confined to the multiples of 360 Hz ( $360 \times 3, 4, 5$ ) near the synchrotron oscillation frequency. Figure 3 shows the sideband frequencies observed at  $\theta_b$ . The solid line in the figure represents the calculated synchrotron oscillation

frequencies at  $\theta_b$ , assuming a designed momentum compaction factor of  $\alpha = 1.46 \times 10^{-4}$ .

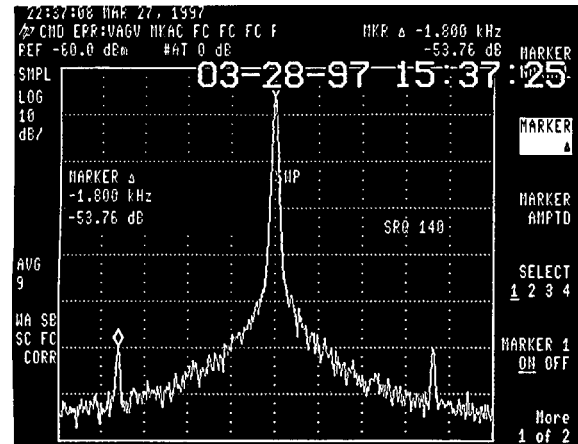


Figure 2: An example of spectrum data taken at  $\theta_b = 18^\circ$ . Large peak in the center is the accelerating frequency (508.58 MHz); and the sideband peaks are observed clearly at the multiple of 360 Hz (1.8 kHz).

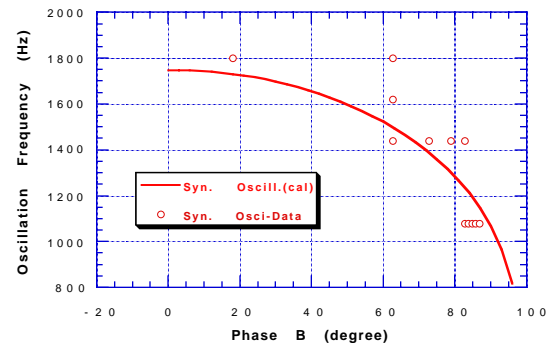


Figure 3: Frequencies of the sideband are plotted as a function of  $\theta_b$ . Circles indicate the observed peak frequencies and the line is the calculated synchrotron frequency.

The intensity of the sideband signals at 1.08, 1.44, and 1.8 kHz, divided by that of the accelerating frequency, are plotted at the corresponding synchrotron oscillation frequencies in Fig. 4.

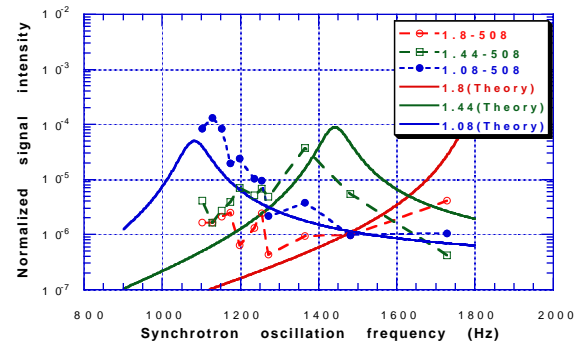


Figure 4: Sideband signal intensities at 1.08, 1.44, and 1.8 kHz. The squares, circles and solid circles represent data at 1.08, 1.44 and 1.8 kHz, respectively. Three curves are calculated using the forced oscillation model (eq 4).

The lines in the figure are calculated from the forced oscillation model. Chain, dotted, and solid lines are

calculated using  $\omega$  in eq(4) set to  $2\pi \times 1080$ ,  $2\pi \times 1440$ , and  $2\pi \times 1800$ , respectively. This model reproduces these sideband amplitude fairly well. Synchrotron oscillation amplitude is calculated using eq(9) and maximum amplitude is  $1.2^\circ$ . Slight shift in peak position comes from the calibration error.

## 5.2 Second measurement

As the first measurement was performed at the early commissioning stage, diagnostic system is not fully equipped. Phase oscillation measuring system was installed and the schematic diagram is shown in Fig. 5. Phase oscillation signal is analyzed using phase detector and FFT analyzer.

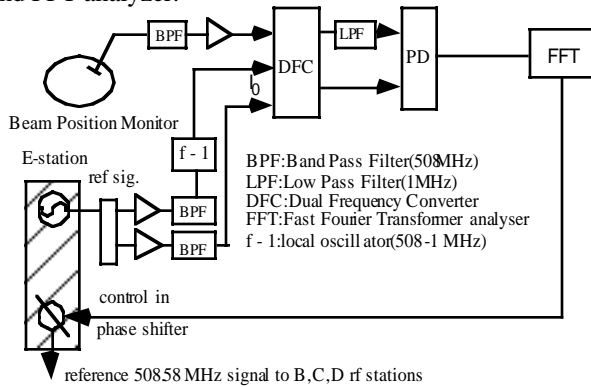


Figure 5: Synchrotron tune measuring system.

In this measurement, effective cavity voltage is changed by changing one RF station voltage keeping the other constant. Phase oscillation signal at multiples of 360 Hz was measured and their intensities are plotted as a function of the synchrotron oscillation frequency in Fig. 6.

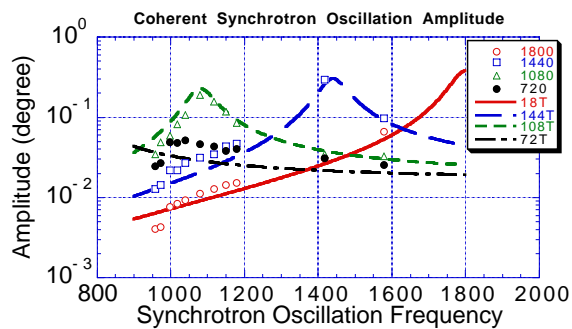


Figure 6: Phase oscillation signal intensities at 720, 1080, 1440 Hz are plotted vs  $f_s$  ( $V_c = V_d = 4$  MV and  $V_b$  varied). Stored current is 1 mA. Curves in the Figure are calculated using eq(4) and assuming that the source intensity at each frequency is the same.

In order to check the two method, spectrum data of the BPM electrode and the phase oscillation signal are taken in the same condition ( $V_b = V_c = V_d = 4$  MV). Coherent synchrotron oscillation amplitude of 1.44 kHz calculated from these data are  $0.18^\circ$  and  $0.13^\circ$ .

From Fig. 4, maximum intensity ratio is measured to be about  $10^{-4}$  at 1080 Hz sideband. The coherent synchrotron oscillation amplitude can be estimated using

eq (9). The maximum forced coherent synchrotron oscillation amplitude corresponding to the intensity ratio is 2 mm while the nominal bunch length is estimated to be about 4 mm. In Fig. 6, synchrotron oscillation frequency was measured using phase oscillation system. Therefore the peak position could well reproduced by the forced oscillation model. Maximum amplitude in Fig. 6 is  $0.6^\circ$  at 1.44 kHz which corresponds to bunch length of 1 mm.

## 6 DISCUSSION

RF low power system of the storage ring has an automatic level control (ALC) and phase lock loop (PLL), and the performance of these control loop was measured [6]. The feedback loops were effective below 1 kHz but not above 1 kHz. In order to reduce the ripple effects, it is necessary to fine tune each power supply and balance the three stations; and to improve the feedback system so that it can adapt to a wider frequency range.

In conclusion, sideband signals from the accelerating frequency were measured by varying the effective cavity voltage. The measured sideband frequencies were multiples of 360 Hz. The characteristics of the signal are fairly well explained by a simple forced oscillation model. Though the peak position of the sideband signal in the first measurement is a little bit different from the calculated one, this comes from the errors in calibrating cavity voltage, phase, momentum compaction factor and so on in the early stage of commissioning. The origin of the forced oscillation is the phase modulation rather than amplitude modulation, because the amplitude fluctuation  $\Delta V / V$  of  $1.5 \times 10^{-2}$  and  $3.7 \times 10^{-3}$  is equivalent to the phase fluctuation  $\Delta \theta_D$  of  $0.85^\circ$  and  $0.2^\circ$ , which is much smaller than the phase modulation itself [6].

## 7 ACKNOWLEDGMENT

The author wish to thank Drs. S. Takano, M. Masaki, S. Sasaki, and other members of the commissioning and operation group of SPring-8 for the data taking, Dr. Y. Miyahara for his helpful discussion and preparation for the manuscript, and the member of RF group for useful discussion.

## REFERENCES

- [1] Schin Daté, Kouichi Soutome, Ainosuke Ando, NIM A355(1995) 199-207.
- [2] M. Hara, T. Nakamura, and T. Ohshima, KEK Proceedings 97-17 Dec. 1997A(MBI97), pp263-272.
- [3] Mathew Sands, "The physics of electron storage rings an introduction"
- [4] J.L. Laclare, "Bunched Beam Coherent Instabilities", CERN 87-03, 21 April 1987.
- [5] N. Kumagai, C. Yamazaki, and H. Kouzu : "Star-point Control for the Klystron Power Supply in the SPring-8 Storage Ring", Proc. Int. Power Electronics Conf., Yokohama, p1497 (1995).
- [6] Y. Ohashi et.al., SPring-8 Annual Report, 161 (1996)